Superdeformation in the $N = Z$ Nucleus ^{36}Ar: Experimental, Deformed Mean Field, and Spherical Shell Model Descriptions

C. E. Svensson,[1] A. O. Macchiavelli,[1] A. Juodagalvis,[2] A. Poves,[3] I. Ragnarsson,[2] S. Åberg,[2] D. E. Appelbe,[4] R. A. E. Austin,[4] C. Baktash,[5] G. C. Ball,[6] M. P. Carpenter,[7] E. Caurier,[8] R. M. Clark,[1] M. Cromaz,[1] M. A. Deleplanque,[1] R. M. Diamond,[1] P. Fallon,[1] M. Furlotti,[9] A. Galindo-Uribarri,[5] R. V. F. Janssens,[7] G. J. Lane,[1] I. Y. Lee,[1] M. Lipoglavsek,[5] F. Nowacki,[10] S. D. Paul,[5] D. C. Radford,[5] D. G. Sarantites,[9] D. Seweryniak,[7] F. S. Stephens,[1] V. Tomov,[9] K. Vetter,[1] D. Ward,[1] and C. H. Yu[5]

[1]*Nuclear Science Division, Lawrence Berkeley National Laboratory, Berkeley, California 94720*
[2]*Department of Mathematical Physics, Lund Institute of Technology, S-22100 Lund, Sweden*
[3]*Departamento de Física Teórica, Universidad Autónoma de Madrid, E-28049 Madrid, Spain*
[4]*Department of Physics and Astronomy, McMaster University, Hamilton, Canada L8S 4M1*
[5]*Physics Division, Oak Ridge National Laboratory, Oak Ridge, Tennessee 37831-6371*
[6]*TRIUMF, 4004 Wesbrook Mall, Vancouver, British Columbia, Canada V6T 2A3*
[7]*Argonne National Laboratory, Argonne, Illinois 60439*
[8]*Institut de Recherches Subatomiques, IN2P3-CNRS-Université Louis Pasteur, F-67037 Strasbourg Cedex 2, France*
[9]*Chemistry Department, Washington University, St. Louis, Missouri 63130*
[10]*Laboratoire de Physique Theorique, Université Louis Pasteur, F-67084 Strasbourg Cedex, France*

(Received 8 May 2000)

A superdeformed rotational band has been identified in ^{36}Ar, linked to known low-spin states, and observed to its high-spin termination at $I^\pi = 16^+$. Cranked Nilsson-Strutinsky and spherical shell model calculations assign the band to a configuration in which four pf-shell orbitals are occupied, leading to a low-spin deformation $\beta_2 \approx 0.45$. Two major shells are active for both protons and neutrons, yet the valence space remains small enough to be confronted with the shell model. This band thus provides an ideal case to study the microscopic structure of collective rotational motion.

PACS numbers: 21.10.Re, 21.60.Cs, 23.20.Lv, 27.30.+t

The microscopic description of collective motion is a fundamental challenge in quantum many-body physics. A classic example in the field of nuclear structure is the desire to understand, within a spherical shell model framework, the origins of nuclear deformation and collective rotation. For deformed nuclei in the first half of the sd shell, this is accomplished in Elliott's SU(3) model [1]. For heavier nuclei, SU(3) symmetry is destroyed by the strong spin-orbit interaction and the relevant coupling scheme is less clear. The microscopic degrees of freedom contributing to the rotational motion can be determined by comparing experimental data, the intuitive results of deformed mean field calculations, and rigorous shell model (SM) diagonalizations. However, the contradictory requirements of having a sufficiently large number of active particles for collective rotation to develop, and a sufficiently small number to permit SM calculations, severely limit the opportunities for such direct comparisons. Considerable effort has recently been focused on ^{48}Cr [2–9], in large part because it is one of a few nuclei where these criteria are satisfied. Rotors like ^{48}Cr are, however, the exception rather than the rule, in that particles from only a single major shell are active, whereas rotational motion in heavier nuclei quite generally involves two major shells for both protons and neutrons.

In this Letter, we report the observation of a superdeformed (SD) rotational band in the $N = Z$ nucleus ^{36}Ar. Cranked Nilsson-Strutinsky and spherical shell model calculations lead to a configuration assignment in which four particles are promoted to the pf shell. This band thus provides an ideal opportunity to extend the microscopic description of collective rotation from the single-shell rotors like ^{20}Ne, ^{24}Mg, and ^{48}Cr to a case involving the cross-shell correlations characteristic of rotational motion in heavier nuclei. The detailed spectroscopic data for the ^{36}Ar band should also provide constraints on the effective sd-pf cross-shell interactions important for the onset of deformation in the neutron-rich "island of inversion" around ^{32}Mg [10,11].

High-spin states in ^{36}Ar were populated via the ^{24}Mg(^{20}Ne, 2α)^{36}Ar reaction, with an 80-MeV ^{20}Ne beam provided by the ATLAS facility at Argonne National Laboratory directed onto a 440 μg/cm^2 ^{24}Mg foil. Gamma rays were detected with 101 HPGe detectors of the Gammasphere array [12], in coincidence with charged particles detected with the Microball [13], a 4π array of 95 CsI(Tl) scintillators. A total of 775×10^6 γ-γ-γ and higher-fold coincidences were recorded during the experiment. The Hevimet collimators were removed from the HPGe detectors to enable γ-ray multiplicity and sum-energy measurements for each event [14], and the ^{36}Ar evaporation channel was cleanly selected by applying energy conservation requirements [15] to events in which two alpha particles were detected.

Here we focus on the identification of a superdeformed band in ^{36}Ar. The γ-ray spectrum obtained by summing coincidence gates set on all members of this band is

shown in Fig. 1(a), and a partial decay scheme for ^{36}Ar is presented in Fig. 2. Transitions denoted by diamonds in Fig. 1(a) firmly link the band to known low-spin states. For example, Fig. 1(b) shows a spectrum of the band obtained with a single gate set on the 4950-keV linking transition. The spin and parity assignments in Fig. 2 are based on angular distribution measurements which establish stretched-$E2$ character for all of the in-band and high-energy linking transitions. Two examples are shown in Figs. 1(c) and 1(d). Legendre polynomial fits to these data (solid curves) yield (a_2, a_4) coefficients of $(0.31 \pm 0.02, -0.09 \pm 0.03)$ and $(0.31 \pm 0.02, -0.08 \pm 0.02)$ for the 3352 and 4166-keV γ rays and establish the 6^+ and 4^+ states of the band. The 4951 keV 2^+ state was known from earlier ^{35}Cl$(p, \gamma)^{36}$Ar studies [16]. These studies also identified a (0^+) state at 4329 keV which, based on the regular rotational spacing, is presumed to be the SD bandhead. The γ-ray branchings from the 4^+ and 6^+ states of the band yield in-band to decay-out $B(E2)$ ratios of 148 ± 6 and 86 ± 4, consistent with strongly enhanced in-band transitions. Assuming a similar ratio of $B(E2)$'s for the 2^+ state, a 622-keV $2^+ \rightarrow 0^+$ in-band transition would be expected to carry $\sim$0.3% of the decay intensity. The present experiment yields an upper limit of 1.0% for this unobserved branch.

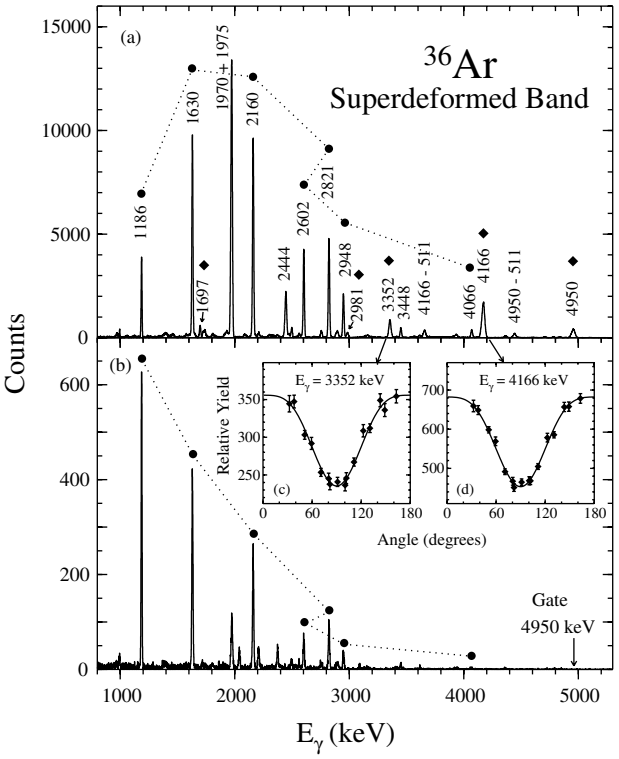

FIG. 1. Gamma-ray spectra obtained by (a) summing coincidence gates set on all transitions in the ^{36}Ar superdeformed band (circles), and (b) setting a single gate on the 4950-keV transition. Diamonds in (a) indicate linking transitions. Angular distributions measured relative to the beam axis are shown for the (c) 3352-keV and (d) 4166-keV transitions.

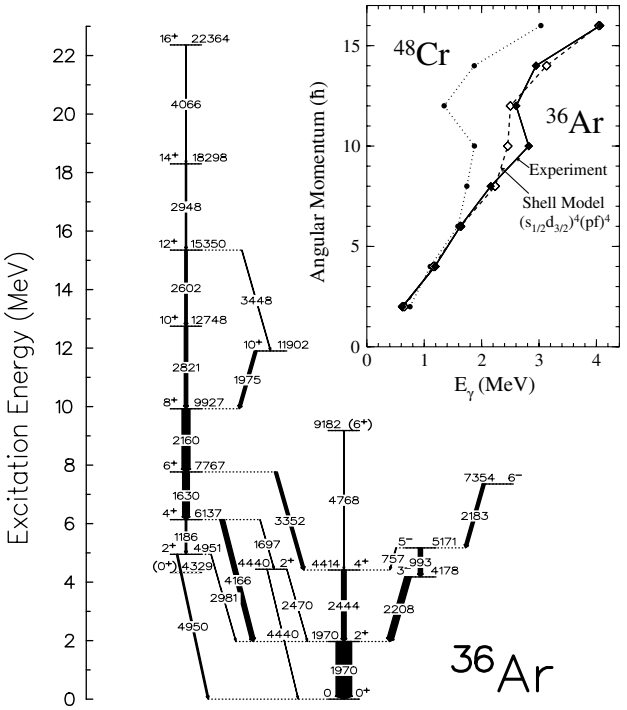

FIG. 2. Partial decay scheme for ^{36}Ar showing the superdeformed band (left). Transition and level energies are given to the nearest keV and arrow widths are proportional to transition intensities. The inset compares the experimental and shell model "backbending" plots for the SD band in ^{36}Ar, as well as experimental values for the ground band of ^{48}Cr [2–4].

The near-perfect rotational behavior of the ^{36}Ar band up to $I = 10\hbar$ is illustrated by the linear increase in angular momentum with rotational frequency (γ-ray energy) shown in the inset in Fig. 2. The data for the ground band of ^{48}Cr [2–4], with low-spin deformation $\varepsilon_2 \approx 0.25$, are also shown for comparison. We note that (i) up to the backbend, the rotational behavior in the ^{36}Ar band is even better than that of ^{48}Cr, and (ii) despite the considerable change of mass, the low-spin moments of inertia are comparable, implying a larger deformation and/or quenching of pairing correlations for the ^{36}Ar band. The maximum spin available in the $(s_{1/2}d_{3/2})^4(pf)^4$ configuration in ^{36}Ar is $I^\pi = 16^+$, and the high-energy γ ray from the 16^+ state suggests a band termination similar to that at $I = 16^+$ in the $(f_{7/2})^8$ configuration of ^{48}Cr [7].

A highly deformed band in ^{36}Ar, in which four pf-shell orbitals are occupied, can readily be inferred from the gap in the energy levels of the Nilsson diagram at deformation $\varepsilon_2 \sim 0.4$ for particle number $N, Z = 18$. This configuration is obtained from the harmonic oscillator SD shell gap at $N, Z = 16$, $\varepsilon_2 = 0.6$ [17] by adding two protons and two neutrons to the upsloping [202]5/2 Nilsson orbital, in a manner analogous to SD shell gaps in heavier nuclei obtained by adding particles to flat or upsloping orbitals above the harmonic oscillator gaps. In this sense, we refer to the ^{36}Ar band as superdeformed. To formalize these ideas, we have performed configuration-dependent [18] cranked Nilsson-Strutinsky (CNS) calculations for

^{36}Ar. The sd-shell Nilsson parameters of Ref. [19] have been adopted and pairing correlations have been neglected. The calculated energies of favored configurations in ^{36}Ar are compared with the experimental data in Fig. 3. The $\pi(pf)^2 \otimes \nu(pf)^2$ configuration, labeled $[2,2]$ in Fig. 3(b), clearly provides the best description of the observed band. Although pairing correlations are known to affect the moment of inertia, and their absence in these calculations leads to the expected discrepancy between the experimental and CNS low-spin slopes seen in Fig. 3, they do not strongly modify the structure of the wave function [6,8]. The CNS calculations are thus expected to provide a reliable description of quadrupole properties [7]. At low spin, a prolate shape with deformation $\varepsilon_2 \approx 0.40$ ($\beta_2 \approx 0.45$) is calculated, and this intrinsic shape remains approximately constant up to $I = 8\hbar$. At higher spins the nucleus is predicted to change shape smoothly (increasing γ at roughly constant $\varepsilon_2 \sim 0.4$), terminating at $I^\pi = 16^+$ in a noncollective oblate ($\gamma = 60°$) state.

We have carried out large-scale sd-pf SM calculations for ^{36}Ar with the diagonalization code ANTOINE [20] and an effective interaction based on that of Ref. [21]. The entire pf shell was included and, following the arguments of Ref. [10], separate calculations were performed with $n = 0$, 2, and 4 particles promoted to this shell. The resulting yrast lines are shown in Fig. 3(c). For $n = 0$, the complete $(sd)^{20}$ space is readily diagonalized and accurately reproduces the observed ground-state band, including the (6^+) state identified in this work. For $n = 2$ and 4, the model space becomes prohibitively large, and for these calculations a closed $d_{5/2}$ orbital was assumed. To account for this truncation, the effective single-particle energies in ^{17}O were adjusted to give the proper level spacings in ^{29}Si and the cross-shell monopole interaction was modified to obtain the correct spectrum for ^{41}Ca. As can be seen in Fig. 3 and in the inset of Fig. 2, these calculations support the $(pf)^4$ assignment for the ^{36}Ar band and provide a truly remarkable description of the data. Even the slight discrepancy for the 10^+ level can, at least partially, be attributed to an interaction between this state and the nearby yrast 10^+ state at 11 902 keV. The latter is a strong candidate for the low-lying 10^+ state belonging to the $n = 2$ configuration which is predicted by both the SM and CNS calculations.

Given the success of both models in reproducing the experimental data, a detailed comparison of these complementary descriptions is of considerable interest. Figure 4 shows the calculated occupancies of spherical j shells for the SD band. The CNS values have been obtained according to the formalism of Ref. [22]. We note that the approximate constancy of the subshell occupancies at low spin validates the concept of a rotational band built on a fixed intrinsic state. At higher spins, the increasingly rapid variations in the occupancies are associated with the predicted change in the intrinsic deformation from prolate to oblate. For the pf shell, the occupancy trends from the

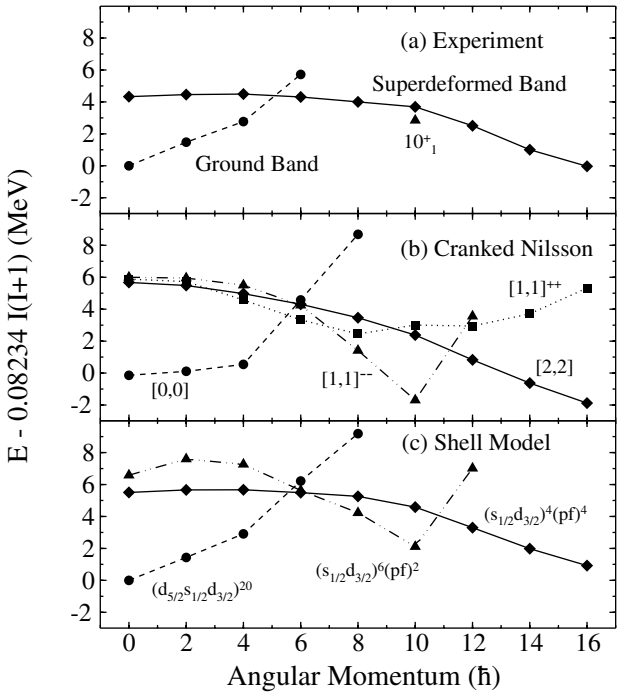

FIG. 3. Energies of positive parity, even spin states in ^{36}Ar relative to a rigid rotor reference from (a) experiment, (b) cranked Nilsson-Strutinsky (CNS), and (c) spherical shell model calculations. The CNS configurations are labeled by $[p,n]$, where p (n) is the number of proton (neutron) pf-shell orbitals occupied and superscripts indicate the signatures of odd sd-shell protons and neutrons.

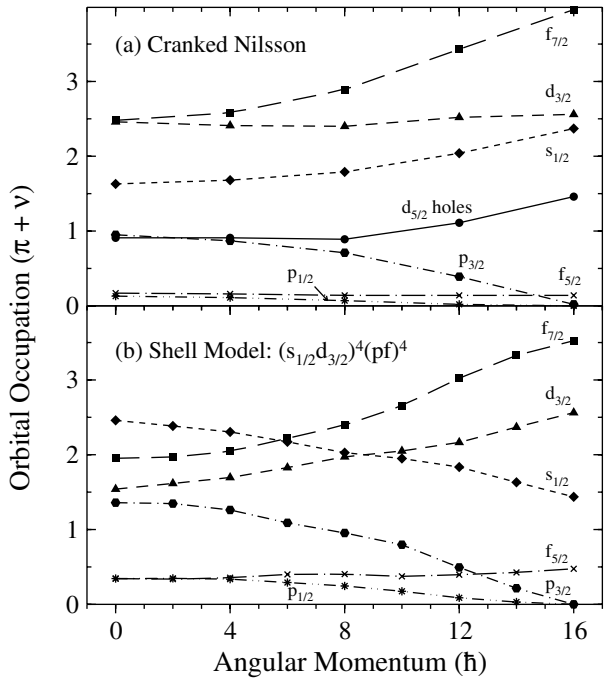

FIG. 4. Occupancies of spherical j shells in the ^{36}Ar superdeformed band from (a) cranked Nilsson-Strutinsky and (b) spherical shell model calculations. In the Nilsson calculations there are also small occupancies in higher major shells.

two approaches are very similar, indicating the dominance of quadrupole deformation in determining the structure of the wave function. The full shell-model treatment of all residual interactions leads to only a slight increase in the upper pf-shell occupancies relative to the deformation-related mixing included in the CNS calculations. It has been noted [23] that with a small number of particles in the pf shell, quadrupole properties can be largely accounted for considering only the favored $\Delta j = 2$ orbitals $f_{7/2}$ and $p_{3/2}$. The $f_{5/2}$ and $p_{1/2}$ orbitals do, however, lead to a significant decrease of the moment of inertia and their inclusion in the SM space is essential to obtain the quantitative agreement with the experimental data seen in Figs. 2 and 3.

In the sd shell, the truncation of the SM space to $(s_{1/2}d_{3/2})$ leads to different occupancy predictions in the two methods. As shown in Fig. 4(a), the CNS calculations, which provide a full description of the j-shell mixing associated with deformation, predict a substantial admixture of $d_{5/2}$ holes in the ^{36}Ar SD band. The near-perfect agreement between experiment and the SM calculation, which does not include the $d_{5/2}$ orbital, suggests that its influence has been largely accounted for by the 1-MeV lowering of the effective $s_{1/2}$ energy in ^{17}O required to reproduce the ^{29}Si spectrum in the modified space. It is also noteworthy that the quadrupole collectivity predicted by the SM calculation is in good agreement with the deformation predicted by the CNS calculation. Assuming $K = 0$, an approximately constant intrinsic quadrupole moment $Q_0 = 113\ e\ \mathrm{fm}^2$ (corresponding to $\beta_2 = 0.45$) is obtained from both the SM spectroscopic quadrupole moments and the calculated $B(E2)$'s connecting low-spin members of the band. This quadrupole moment represents 80% of the maximum available in the $(sd)^{16}(pf)^4$ space [as attained in the unrealistic SU(3) limit], and we therefore expect that including the $d_{5/2}$ orbital in the SM space would not increase the quadrupole moment by more than 5%–10%. A complete study of the role of the $d_{5/2}$ orbital in the microscopic structure of the ^{36}Ar SD band, perhaps through a full sd-pf diagonalization by Monte Carlo SM techniques (cf. Ref. [24]), would, of course, be of great interest. Such a calculation would also provide information regarding the mixing of configurations with different numbers of pf-shell excitations necessary for a complete understanding of the decay out of the band and the interaction of the two 10^+ states in Fig. 2. From the deformed mean field perspective, a full treatment of pairing correlations would provide additional insight into the relative contributions of deformation and pairing to the j-shell occupancies and, conversely, the SM occupancies could be used to test, and improve upon, the standard pairing approximations. Experimentally, lifetime measurements for states in the ^{36}Ar SD band will provide stringent tests of the quadrupole properties predicted by both models.

In summary, we have identified a superdeformed rotational band in the $N = Z$ nucleus ^{36}Ar. The band is linked to low-spin levels and is observed to its termination at $I^\pi = 16^+$. Cranked Nilsson-Strutinsky and large-scale shell model calculations lead to a configuration assignment involving the occupation of four pf-shell orbitals and predict a low-spin quadrupole deformation $\beta_2 \approx 0.45$. With two major shells active for both protons and neutrons, yet a valence space dimension small enough to be approached from the shell model perspective, this band provides an ideal test case for further studies of the microscopic description of rotational motion in nuclei.

We thank W. E. Ormand for helpful discussions. This work has been partially supported by the DOE under Contracts No. DE-AC03-76SF00098, No. W-31-109-ENG-38, No. DE-AC05-96OR22464, and No. DE-FG05-88ER40406, the Swedish Institute, NFR (Sweden), DGES (Spain) under Grant No. PB96-53, NSERC (Canada), and IN2P3 (France).

[1] J. P. Elliott, Proc. R. Soc. London **245**, 128 (1958); **245**, 562 (1958).
[2] J. A. Cameron *et al.,* Phys. Lett. B **387**, 266 (1996).
[3] S. M. Lenzi *et al.,* Z. Phys. A **354**, 117 (1996).
[4] F. Brandolini *et al.,* Nucl. Phys. **A642**, 387 (1998).
[5] E. Caurier *et al.,* Phys. Rev. C **50**, 225 (1994).
[6] E. Caurier *et al.,* Phys. Rev. Lett. **75**, 2466 (1995).
[7] A. Juodagalvis and S. Åberg, Phys. Lett. B **428**, 227 (1998); A. Juodagalvis, I. Ragnarsson, and S. Åberg, Phys. Lett. B **477**, 66 (2000).
[8] A. Poves, J. Phys. G **25**, 589 (1999).
[9] K. Hara, Y. Sun, and T. Mizusaki, Phys. Rev. Lett. **83**, 1922 (1999).
[10] E. K. Warburton, J. A. Becker, and B. A. Brown, Phys. Rev. C **41**, 1147 (1990).
[11] T. Motobayashi *et al.,* Phys. Lett. B **346**, 9 (1995); E. Caurier *et al.,* Phys. Rev. C **58**, 2033 (1998); D. J. Dean *et al.,* Phys. Rev. C **59**, 2474 (1999).
[12] I.-Y. Lee, Nucl. Phys. **A520**, 641c (1990).
[13] D. G. Sarantites *et al.,* Nucl. Instrum. Methods Phys. Res., Sect. A **381**, 418 (1996).
[14] M. Devlin *et al.,* Nucl. Instrum. Methods Phys. Res., Sect. A **383**, 506 (1996).
[15] C. E. Svensson *et al.,* Nucl. Instrum. Methods Phys. Res., Sect. A **396**, 228 (1997).
[16] P. M. Johnson, M. A. Meyer, and D. Reitmann, Nucl. Phys. **A218**, 333 (1974).
[17] R. K. Sheline, I. Ragnarsson, and S. G. Nilsson, Phys. Lett. **41B**, 115 (1972).
[18] T. Bengtsson and I. Ragnarsson, Nucl. Phys. **A436**, 14 (1985); A. V. Afanasjev and I. Ragnarsson, Nucl. Phys. **A591**, 387 (1995).
[19] D. M. Headly, R. K. Sheline, and I. Ragnarsson, Phys. Rev. C **49**, 222 (1994).
[20] E. Caurier, computer code ANTOINE, CRN, Strasbourg, 1989.
[21] J. Retamosa *et al.,* Phys. Rev. C **55**, 1266 (1997).
[22] R. K. Sheline *et al.,* J. Phys. G **14**, 1201 (1988).
[23] A. P. Zuker *et al.,* Phys. Rev. C **52**, R1741 (1995).
[24] T. Otsuka, M. Honma, and T. Mizusaki, Phys. Rev. Lett. **81**, 1588 (1998).